Investigation of Sweep Configuration Effects on Propeller Performance

Shohei Nomura, Craig Paxton, Wai (Winola) Cheong
Peter Gryn, GeCheng Zha

Dept. of Mechanical Engineering
University of Miami
Coral Gables FL 33124
Contact: zha@apollo.eng.miami.edu

Abstract

The objectives of this research are to study the effects of propeller sweep and to find the optimal sweep configurations. At this point, one straight propeller and one swept propellers have been simulated. Further CFD analyses on other propeller configurations are in progress and will be reported in the final paper.

1. Introduction

The idea of a swept propeller first began in Germany in the 1930s. After War World II, much effort was made to design aft swept propeller blades. In the late 1970's, NASA focused on single rotation propellers by using an axial backward aerodynamic sweep.[1,2,3,4,5,6] Significant improvement in efficiency and noise reduction were achieved at high subsonic Mach numbers of between 0.7 and 0.8.[6]

Since then, many efforts were made to employ backward aerodynamic sweep technology in order to improve efficiency and stall margin characteristics.[9] However, no break through using any type of sweep was achieved until GE Aircraft Engines announced in 1998 that they had succeeded in using forward sweep to improve the stall margin and efficiency of a two-stage fan.[9]

The possible mechanisms that cause the better performance are that the tip of a forward swept blade touches "clean air" first (non-turbulent air), it is then able to pull more mass flow and has higher flow kinetic energy, which helps to suppress the tip vortex. The turbulence intensity in the tip-end wall boundary layer is also likely to be lower and would therefore generate less noise.

The research of this paper is a continuation of the research on high efficiency forward swept propellers, with a new concentration studying the optimal sweep configuration. Based on the CFD simulation results and wind tunnel testing from previous research, it was proved that forward swept propellers yielded high efficiency than the straight propeller[12, 14]. Therefore, a few direct forward swept propellers have been studied in order to find the optimal forward swept angle. Different leading edge configurations are being studied and the investigation of the optimal sweep configurations will be reported for the final paper.

2. Aerodynamic Designs

Research on forward swept propellers at low Reynolds numbers has shown promise of increasing efficiency and stall margin.[12] The same forward sweep design concept was used for this research, in which the forward sweep was solely achieved by a tangential lean of the blade's leading edge towards the rotation direction. This was done by keeping the leading edge at a constant axial position across the entire blade span. For the current research, when the leading edge position is determined, the airfoil is stacked along the leading edge, parallel to the horizontal line.

Due to the constraints of manufacturing and test facilities available for this research, propellers were designed to operate in the incompressible region with a maximum Mach number of 0.3 at a Reynolds number of approximately 100,000.

The propellers studied in this research are two blade propellers with a diameter of 155mm. The reference propeller is a straight blade Graupner 5.9"x 5.9" CAM speed propeller, which is able to fly at a cruise velocity of 27 m/s at 12,100 RPM. Since all propellers were made to mimic the performance of this reference propeller, all designed blades, straight and swept, have the same chord and thickness values at identical radii as the Graupner blade.

According to past researches, R.A.F.-6 and Clark Y are the most commonly used airfoils in propeller designs with the Clark Y being preferred by propeller deisgners.[11] The R.A.F.-6 airfoil performs better at climb and take-off for high-speed planes, but the Clark Y airfoil produces higher peak efficiencies on low-pitch propellers with overall efficiency increasing as blade thickness increases[11]. The Clark Y provides substantial lift at low speeds and gentle stall characteristics. Due to the above reasons, Clark Y was selected for the research.

There are three types of sweep configurations, which are discussed in detail in the Design Tool section of this abstract. At this point, the current research is focused on the direct forward sweep design, the study of other configurations is in progress.

3. Design Tool

A computer program was developed in order to make the design process more flexible and less time consuming. The program is capable of instantly generating the coordinates of propeller blades with different design configurations. The design options include the operating conditions (RPM, cruise velocity, angle of attack), with a user specified leading edge geometry (figure 1) and airfoil alignment type (figure 2)

Leading edge geometry includes straight, direct sweep, delayed sweep, and combined sweep. The direct sweep configuration was constructed by extending the leading edge from r_{root} with a constant sweep angle ψ until it intersects r_{tip} (figure 3). The delayed sweep configuration was constructed by leaning the leading edge in the direction of rotation at a distance ξ away from r_{root} (figure 4). The combined sweep configuration was constructed by joining the backward and forward leaning edges with a tangent arc (figure 5).

In this research, the main focus is on the direct forward sweep option. The rest of the geometries will be explored aiming to locate the optimal sweep angle for each configuration, and also the overall optimal combination of sweep angle and design.

Airfoil alignment types include transfer, translate and transform. In transfer, the airfoil at each section is aligned parallel to the horizontal line; there is no rotation on the airfoil. In other words, all blades with this alignment type were designed so that the airfoils are exactly the same at identical radial locations. This would ensure that the difference in performance was due solely to the sweep effect. In transform (figure 6), the airfoil at each section is rotated and aligned with the local flow direction. In translate (figure 7), the airfoil is rotated and aligned normal to the leading ledge. The current research is using the transfer option, where airfoil is aligned parallel to the horizontal line. The other two options will be explored and their causes and effects on the performances of the propellers will be studied.

Altogether, over 200 configurations are available through this program. In the final report, more design features will be added to the program, such as the scaling options for the blade, different airfoil selections, and add a graphical user interface. If all of these proposed editions are completed, the program would be capable of generating over 700 unique configurations, which would streamline the propeller design process. Blade Designer generates a coordinate file for input to Pro/Engineer where 3D models are obtained, these models are then used for CFD mesh generations.

4. CFD

Figure 8 shows the standard computational domain created for CFD simulations. It consists of two domains: an inner and outer domain. The inner domain is the smaller of the two half-cylinders, in which the propeller blade and cone are located (figure 9). The outer domain is the bigger of the two half-cylinders and completely encompasses the

inner domain. The inner and outer domains were assigned the radius of 150mm (approximately 2 blade lengths) and 1600mm (approximately 29 blade lengths), respectively.

The inlet boundary was placed 18 blade lengths in front of the blade and the outlet was placed 18 blade lengths behind the blade. Due to the rotating reference frame, a far-field boundary was established at a constant radius of approximately 29 blade lengths from the blade. These boundary conditions were placed far from the propeller in order to reduce interaction with the flow induced by the propeller and simulate and open air environment. The nosecone of the motor and nacelle (figure 11) were also constructed as part of the CFD model in order to mimic the setup of wind tunnel testing. The nacelle was extended to the outlet in order to simplify the geometry and CFD boundary conditions.

The inlet and far-field zones were assigned as velocity inlet boundary conditions which Fluent describes as a zone where "the total (or stagnation) properties of the flow are not fixed, so they will rise to whatever value is necessary to provide the prescribed velocity bistrubution."[13] The outlet was assigned an outflow boundary condition, which Fluent says "are used to model flow exits where the details of the flow velocity and pressure are not known prior to solution of the flow problem."[13] In other words, no parameters are specified at outflow boundaries; FLUENT extrapolates the required information from the interior. The no-slip boundary condition was used for all walls and the Periodic rotational boundary condition is used for the two horizontal periodic planes.

It can be seen in figure 10 and 11 that the mesh spacing is smaller within the inner domain and coarser in the outer domain. It was desirable to obtain this kind of packed (clustered) mesh in the vicinity of the propeller blade, so that FLUENT (solver) will be able to resolve the wall boundary layer and tip vortices. The purpose of having the two domains is to simplify this meshing process and to localize the finer mesh within complicated flow regions.

In order to achieve a mesh-independent solution, it is necessary to perform a mesh refinement to increase the number of cells and re-simulate. The boundary layer was specially chosen for mesh refinement because the flow is in the region of high velocity gradients. Initially, four boundary layers were applied, and it was increased by one or two layers in each mesh refinement. For example, straight blade was simulated with 4 (figure 12), 6, 7 and 8 (figure 13) boundary layers at the same free stream velocity. Percentage change in the efficiency between each increased boundary layer simulation was calculated to be 15.4%, 0.76% and 0.016%. In all simulations second order discretization scheme is used for the momentum.

5. Preliminary Results

Previous research has experimentally proven, that the forward swept propellers yielded higher efficiency and stall margin.[12] This current research concentrated on the design

optimization to find the optimum angle of sweep for a given configuration and the overall optimal combination of sweep angle and design that yields the best efficiency.

A more enhanced design tool, was successfully developed, allowing the users to generate the coordinates of the blade of different design configurations with ease. At this point, the design tool features the design options of operating conditions, leading edge configurations, and airfoil alignment types. The program then exports a coordinate file to Pro/Engineer so that a 3-D model can be generated.

In order to establish a baseline trend of efficiency the straight blade was simulated. The 20-Forward propeller is shown with the baseline straight in figure 14 and additional configurations will be studied in the near future. Figure 14 shows that 20-Forward actually yielded lower efficiency than the straight blade; these results contradict the wind tunnel testing results from the previous research.[12]

Significant effort has been put into mesh refinement in an attempt to obtain a mesh independent solution. Mesh refinement was repeated until there were eight boundary layers and the percentage change in the steady state solutions fell within 1% (Figure 10).

The cause for the discrepancy between the current results and the results found in the previous research, as well as the appropriate discretization and interpolation schemes will be determined. In order to achieve these goals, further mesh refinement around the blade will be performed and will be simulated with different schemes.

6. Works in progress

Research will continue to be conducted aiming to find the optimum sweep configuration for different blade configurations. More mesh refinement, as well as further study about discretization and interpolation schemes will be done in an attempt to find the appropriate CFD setup. At the same time, propeller manufacturing will also be pursued for wind tunnel testing in order to verify the CFD results. To further verify the reliability of the current CFD setup, backward swept propellers will be simulated and the results will be compared to those of the straight blade.

7. Acknowledgements

We own our deepest and most sincere thanks to the following companies, department and individuals for the assistance they offered.

Fraunhofer Technology Center Hialeah, Department of Industrial Engineering at the University of Miami, Hobby Lobby, DuPont, Sermatech Castings, Florida International University, Stratasys International Inc., University of Florida, Mr. Ryan Holman, NASA Glenn Research Center, Mr. Robert Jeracki

8. References

1. Whitcomb, Richard T. “A Discussion of the Design of Highly Swept Propeller Blades” – NACA RM L50A23. National Advisory Committee for Aeronautics, Washington; May 4, 1950.

2. R. J. Jeracki and G. A. Mitchell, “Low and High Speed Propellers for General Aviation- Performance Potential and Recent Wind Tunnel Test Results”, NASA TM 81745, 1981.

3. R. J. Jeracki, D. C. Mikkelson, and B. J. Blaha, “Wind Tunnel Performance of Four Energy Efficient Propellers Design for Mach 0.8 Cruise”, NASA TM 79124, 1979.

4. G. L. Stefko, and R. J. Jeracki, “Wind-Tunnel Results of Advanced High-Speed Propellers at Takeoff, Climb, and Landing Mach Numbers”, NASA TM 87030, 1985.

5. C. J. Miller and J. P. Sullivan, “Noise Constraints Effecting Optimal Propeller Designs”, NASA TM 86967, 1985.

6. D. C. Mikkelson and G. A. Mitchell, “Summery of Recent NASA Propeller Research”, NASA TM 83733, 1984.

7. Nichols, G. H. “Design and Fabrication of Forward-Swept Counter-rotation Blade Configuration for Wind Tunnel Testing” – GE Advanced Technology Operations. Contract NAS3-25269, CR - 191193. March 1, 1994.

8. R. J. Jeracki, “Private Communication”, NASA Glenn Research Center, April 2, 2002.

9. A.R. Wadia , P.N. Szucs, and D.W. CrallInner, “Inner Workings of aerodynamic Sweep”, ASME Journal of Turbomachinery, Vol. 120, October 1998.

10. G.C.Zha, “Arched Wings: Possible Improvement of the Wing Performance”, AIAA paper-94-0054, 1994.

11. Freeman, Hugh B. Comparisons of Full-Scale Propellers Having R.A.F.-6 and Clark Y Airfoil sections; Langley Memorial Aeronautical Laboratory, NACA; Oct 8, 1930.

12. C. Paxton, P. Gryn, E. Hines, U. Perez, and G.C.Zha, “High Efficiency Forward Swept Propellers at Low Speed”, AIAA 2003-1069

13. *Fluent 6.0 User’s Guide*, Fluent Incorporated, 2002

14. G.C.Zha, C.Paxton, P.Gryn, E.Hines, and U.Perez, “Forward Swept High Efficiency Airplane Propeller Blades”, Patent pending, submitted to USPTO on Dec. 30, 2002

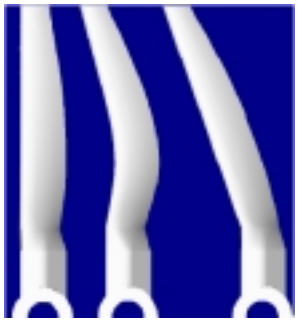

Figure 1: Pro/E propeller geometry

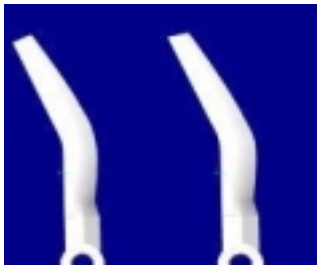

Figure 2: Airfoil alignments of Translate (left) and Transform (right)

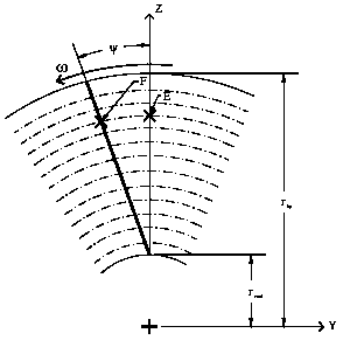

Figure 3: Direct forward swept design configuration

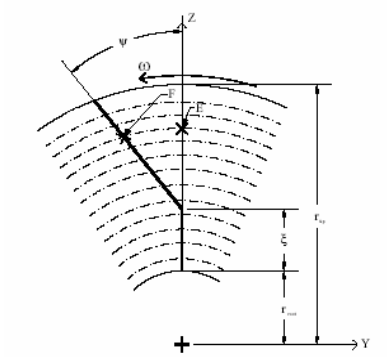

Figure 4: Delayed forward sweep design configuration

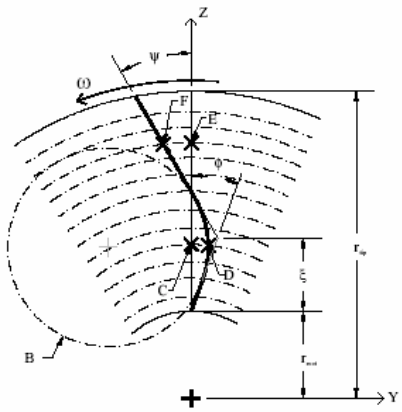

Figure 5: Combined backward-forward swept design configuration

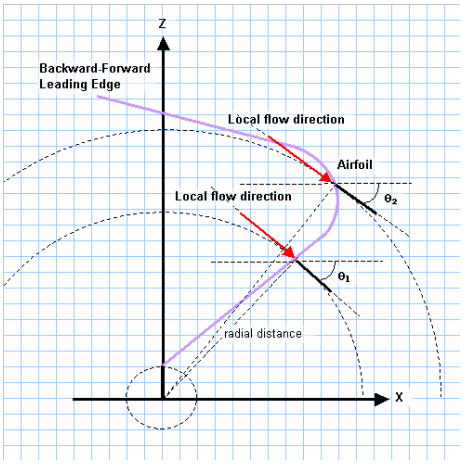

Figure 6: Airfoil Alignment, Transform

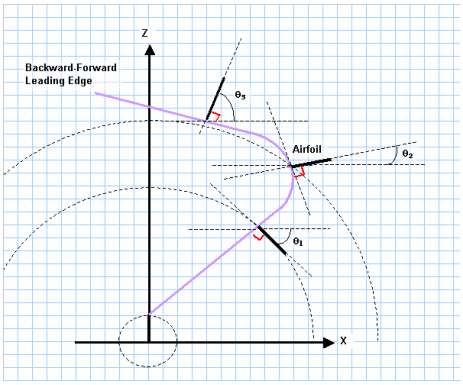

Figure 7: Airfoil Alignment, Translate

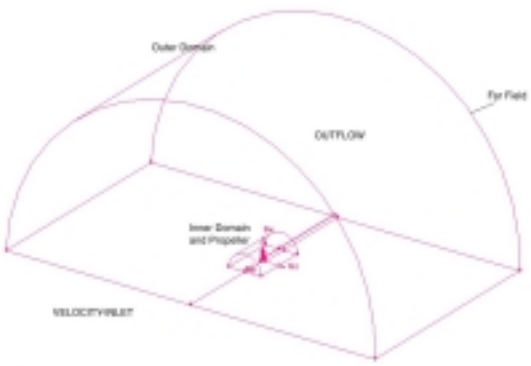

Figure 8: 3-D computational domains

Figure 9: Inner domain

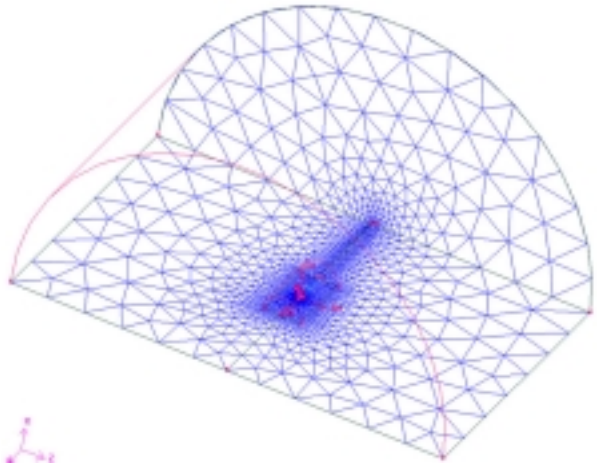

Figure 10: Mesh of the CFD model

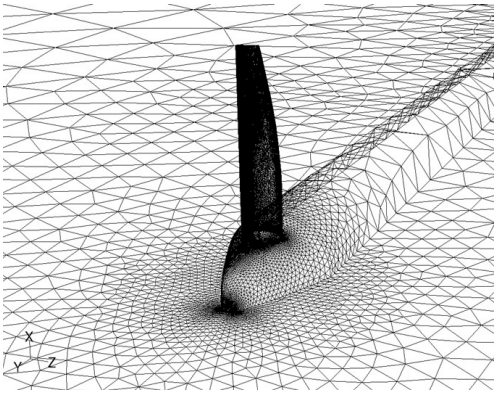

Figure 11: Isometric view of blade, cone, nacelle, and inner periodic faces

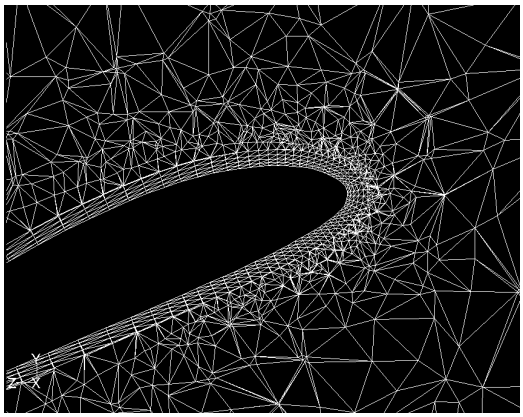

Figure 12: Projection of 3-D mesh onto the cross sectional plane (4 boundary layers)

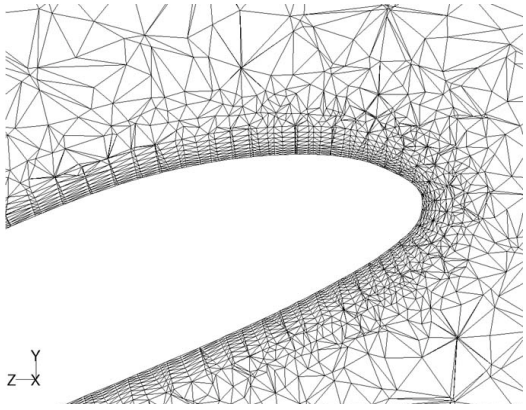

Figure 13: Projection of 3-D mesh onto the cross sectional plane (8 boundary layers)

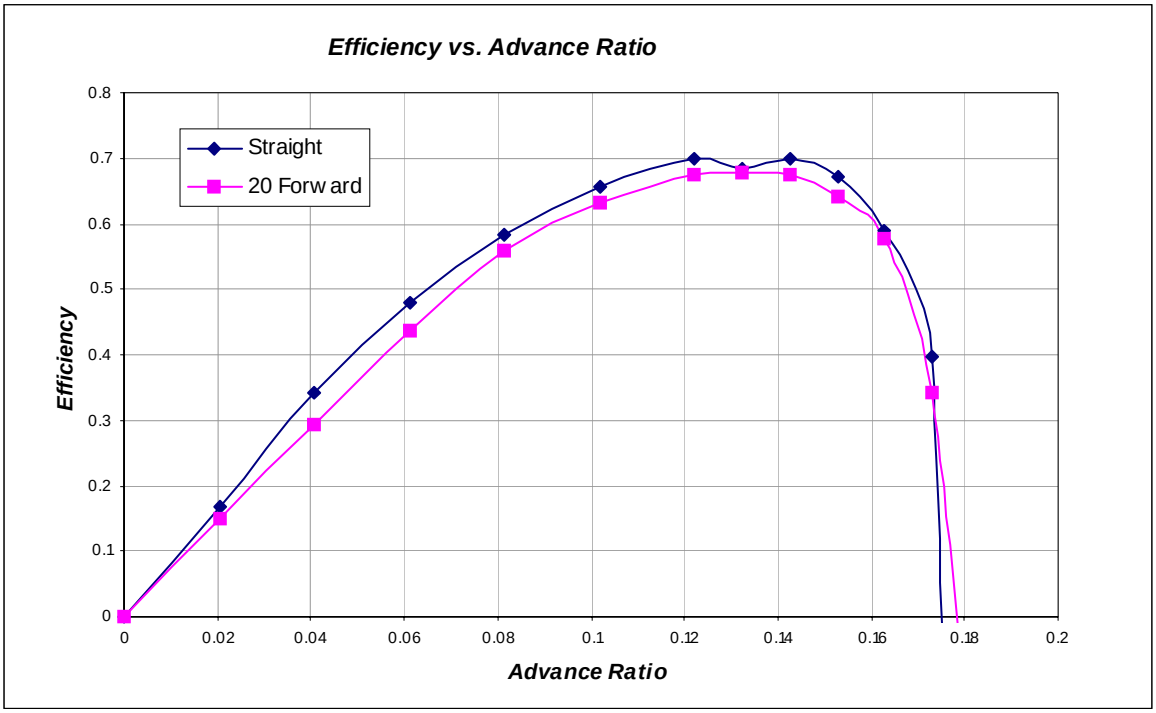

Figure 14: CFD efficiency vs. advance ratio results